Available online at www.sciencedirect.com
ScienceDirect
Journal of Sound and Vibration 308 (2007) 112–131
JOURNAL OF SOUND AND VIBRATION
www.elsevier.com/locate/jsvi

Granular damping analysis using an improved discrete element approach

X. Fang[a], J. Tang[a,*], H. Luo[b]

[a]*Department of Mechanical Engineering, The University of Connecticut, 191 Auditorium Road, Unit 3139 Storrs, CT 06269, USA*
[b]*GE Global Research Center, 1 Research Circle, Niskayuna, NY 12309, USA*

Received 23 June 2006; received in revised form 23 January 2007; accepted 18 July 2007
Available online 30 August 2007

Abstract

Granular damping has promising potential for vibration suppression in harsh environment. Currently, the discrete element method (DEM) is adopted in the granular damping analysis that typically involves a large number of granules. While the discrete element method, which is essentially built upon the direct numerical integration of Newton's equations, has been widely used in various analyses involving granular motion, the granular damping analysis faces unique challenge in several aspects. Unlike many other granular motion analyses, in the granular damping analysis the movements of the granules are strongly coupled with that of the host structure, and the granules experience extremely frequent collisions with each other. Meanwhile, the energy dissipation mechanism is highly nonlinear, and can only be evaluated with sufficiently long simulation time especially for structures vibrating in the low-frequency range. In order to increase the analysis efficiency to enable large-scale parametric studies, in this research we develop a new computational scheme for granular damping analysis using the discrete element approach. The main idea is to enhance the efficiency of contact detection in such analysis. To reduce the number of candidate granular pairs for contact check, an improved link cell (LC) scheme is proposed which takes advantage of the contacting force relation. This is followed by incorporating a Verlet table into the analysis that records all granular pairs whose distances are less than a certain threshold distance. The Verlet table for candidate pairs will be updated in an adaptive manner, corresponding to the dynamic states of the vibrating system. We also study the effect of time step in the numerical simulation, and develop a procedure that can optimize the time-step selection based on the contact mechanics. Collectively, these improvements can increase the computational efficiency of the discrete element method by multiple times as compared to the state-of-the-art. The proposed approach is validated by correlating to benchmark numerical and experimental results. With the new algorithm as basis, case studies are carried out to illustrate the analysis of granular damping mechanisms and the optimization of damping performance.

1. Introduction

Granular damper is a passive vibration control device in which granules of various sizes and materials are inserted into an enclosure embedded within or attached to the primary vibrating structure. Each collision among the granules and between the granules and the enclosure wall leads to energy absorption and

*Corresponding author. Tel.: +1 860 486 5911.
E-mail address: jtang@engr.uconn.edu (J. Tang).

0022-460X/$ - see front matter © 2007 Elsevier Ltd. All rights reserved.
doi:10.1016/j.jsv.2007.07.034

dissipation, resulting in attenuation of the vibratory response [1–3]. Granular damping can provide vibration suppression with a small weight penalty and without significant impact on the strength and stiffness of the structure [1,4,5]. One unique feature of granular damping is that its performance is essentially independent of the environment [5], while many other damping devices, e.g., viscoelastic materials, may lose their effectiveness in harsh environments. For example, tungsten carbide granules can sustain very high temperature ($>2000^\circ$ F) and remain at granular status to effectively provide passive damping [6]. Therefore, granular dampers have been considered for use in high-temperature environments such as turbo-machinery blade applications.

Although simple in concept, the granular damper is very complicated in terms of detailed analysis and design. The granular motion and the associated energy dissipation mechanisms are highly nonlinear and depend on a very large number of system parameters as well as specific operating conditions such as vibration amplitude and frequency, etc. [7]. Indeed, the granular damping results from a combination of several different loss mechanisms such as granule-to-granule impact/collision, granule-to-wall impact, and dynamic frictions, and certain trade-offs exist under a given vibration condition [2]. It has been recognized that the discrete element method, which keeps track of the motion of all granules, can accurately characterize the dynamics of a system involving granules. Since the early work by Cundall and Strack in the field of rock mechanics [8], the discrete element method has been applied to a variety of granular motion analyses and recently to granular damping analyses [9,10]. The discrete element method is a numerical technique based on Newton's equations to model the motion of an assembly of granules interacting with each other. The procedure is an explicit process with small time-step iterations to determine the resultant forces and moments on each granule in the system. Typically, the time steps taken are sufficiently small such that during a single time step the disturbances cannot propagate from any granule further than its immediate neighbors [8]. As a result, at a given time, the resultant forces/moments on any granule are determined exclusively by its interaction with the granules and the host structure with which it is in contact. When applied to granular damping analysis, the discrete element method can yield a complete and accurate description of granular motion inside the damper enclosure, which will lead to quantitative understandings of various energy dissipation mechanisms in both transient and steady-state vibrations [2–5].

The successful implementation of discrete element method for granular motion analysis relies on two important aspects: an accurate force–displacement model characterizing the behavior of granules in contact, and an efficient contact detection algorithm to determine which pairs of granules are in contact [9,11,12]. For the granular damping analysis, a series of studies have been dedicated to the identification and verification of contact mechanics model for typical granular materials, and recent results have shown good agreement between numerical simulations and experimental analyses [4,5]. On the other hand, currently, the main issue in granular damping analysis is the computational efficiency. Particularly, the contact detection, which is one major and time-consuming step in the discrete element method analysis [11], becomes more computationally involved. The underlying mechanism of granular damping is the energy dissipation/absorption through impact/collision. Unlike many other granular motion analyses, in the granular damping analysis the movements of the granules are strongly coupled with that of the host structure through impact, and the granules experience extremely frequent collisions with each other during the structural vibration. Therefore, the relative positions between the granules and between the granules and the enclosure may have significant changes in a very short time period, which necessitates very frequent contact check. Meanwhile, the energy dissipation mechanism of granular damping is highly nonlinear, and can only be analyzed with sufficiently long simulation time. This is especially true for structural vibration in the low frequency range, where oftentimes a simulation time as long as a few seconds is needed to quantitatively evaluate the vibration suppression performance. Moreover, due to the nonlinearity, a very large number of parametric studies have to be carried out to cover the entire operating condition range. Clearly, the efficiency of the discrete element approach needs to be improved, so one may have thorough understanding of granular damping mechanisms through systematic parametric analyses and then perform design and optimization of granular dampers for practical applications.

2. Objective and research overview

The objective of this research is to develop a discrete element-based approach for granular damping analysis with significantly improved computational efficiency. We use a force–displacement model that is based on the

Hertzian contact theory to describe the nonlinear impact phenomenon when the granules are in contact with each other or in contact with the enclosure wall [4,5]. A series of improvements will be incorporated into the discrete element method to enhance the contact detection efficiency. In recent granular motion studies, the link cell (LC) method has shown promising features in limiting the contact detection to granules' neighbors [2,3]. In this research, we improve the LC method by taking into account the contacting force relation, which reduces the number of neighboring cells to be inspected. Following that, a Verlet table [11] is incorporated into the LC method to record all granular pairs whose distances are less than a threshold distance d_t. The combination of LC method and the Verlet table can drastically reduce the number of granular pairs to be checked for potential contact. It is worth mentioning that the Verlet table needs to be dynamically updated to reflect the current granular motion status, and in general the generation of Verlet table could take notable computational effort, especially when the number of granules is large. In this research, we develop an adaptive strategy that is based on the instantaneous dynamic states of granules (e.g., velocity) to reduce the frequency of updating Verlet table. We also study the effect of time-step selection in simulation, and develop a procedure that can optimize the time-step selection based on the contact duration of given granules. Collectively, these new improvements can greatly increase the computational efficiency of the discrete element approach. The improved discrete element method algorithm is then coupled with structural vibration for damping evaluation. Detailed numerical analyses are performed to highlight the accuracy and efficiency of the proposed approach. Using this new algorithm, we also carry out parametric analysis on granular damping to explore its damping mechanisms and the optimization of damping performance under some specific systematic settings.

3. Dynamic equations and contact mechanics

The focus of this research is on the computational efficiency of discrete element method specifically for granular damping analysis. For the completeness of the presentation, in this section the dynamic equations and contact mechanics model used in the discrete element method are briefly outlined. In the discrete element method, the trajectory of each discrete element (granule) is tracked incrementally by Newton's equations of motion. Forces are computed at the contacts among the granules and between the granules and the enclosure wall by suitably describing the contact behavior by means of a force–displacement law. Owing to the collision and friction between two granules or between a granule and the enclosure wall, a granule may have two types of motion: the translation and the rotation. The translational motion is caused by the contact force and gravitational force. The rotational motion is normally caused by the contact forces only. The dynamic equations are given as [13]

$$\begin{aligned} m_i\ddot{\mathbf{p}}_i &= \boldsymbol{f}_i - m_i\mathbf{g} \\ I_i\ddot{\boldsymbol{\theta}}_i &= \mathbf{T}_i \end{aligned} \qquad (i = 1, \ldots, n), \tag{1}$$

where n is the total number of granules, m_i the mass of the ith granule, I_i the moment of inertia of the ith granule, $\mathbf{p}_i$ the position vector of the center of gravity of the granule, $\boldsymbol{\theta}_i$ the angular displacement vector, $\mathbf{g}$ the gravity acceleration vector, $\boldsymbol{f}_i$ the summation of the contact forces acting on granule i from other granules or from the enclosure wall, and $\mathbf{T}_i$ is the summation of torques caused by the contact forces.

When the distance between the centers of two granules is smaller than the summation of their radii, these two granules are in contact and contact forces arise, as shown in Fig. 1(a). In the calculation of the contact forces, the granules are allowed to overlap and every such overlapping contact can be modeled using a spring, dashpot, and slider in the normal and tangential directions shown in Fig. 1(b) [14,15]. Cundall and Strack [8] used a linear model by assuming constant values of stiffness and damping. Numerical and experimental studies [16,17] have shown that the expression of contact force using a linear model may not reflect the contact mechanics accurately, and a nonlinear displacement–force relation exists at the impact area. In this research, we implement the nonlinear contact model proposed in Ref. [14], which has also been used in granular flow and impact engineering with satisfactory results [16]. In Fig. 1(a), $\mathbf{p}_i$ and $\mathbf{p}_j$ denote the positions of the centers of granules i and j, respectively. We consider the normal component, $\boldsymbol{f}_{nij}$, and the tangential component, $\boldsymbol{f}_{tij}$, of the contact force acting on granule i by granule j. The normal component $\boldsymbol{f}_{nij}$ of the contact force can be modeled by the sum of the spring force based on the Hertzian contact theory and the damping force D_n, and is

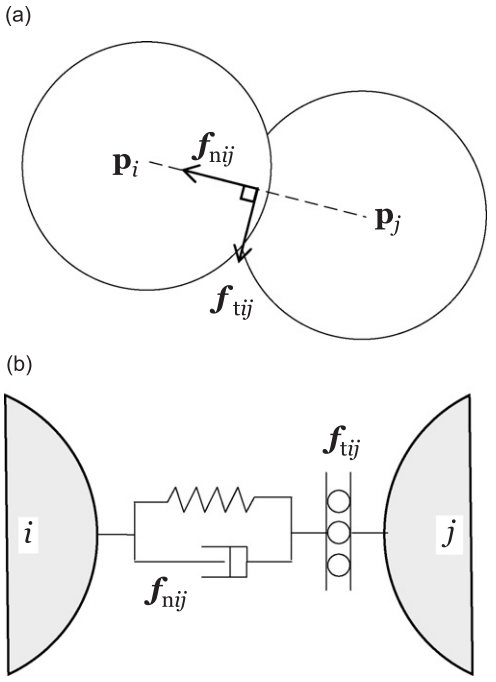

Fig. 1. (a) Contact between granules i and j; (b) sketch of the spring-dashpot model for the collisional normal and tangential forces between granules.

expressed as [4,5,14]

$$\boldsymbol{f}_{nij} = -(k_n \delta_{nij}^{3/2} + D_n)\boldsymbol{n}_{ij}, \tag{2}$$

where δ_{nij} is the normal displacement of granule i relative to granule j, k_n is the spring constant, D_n is the damping force, and $\boldsymbol{n}_{ij}$ is the unit vector from the center of granule i to that of granule j. During the contact between granules i and j, the normal displacement δ_{nij} is given as

$$\delta_{nij} = r_i + r_j - |\mathbf{p}_i - \mathbf{p}_j|, \tag{3}$$

where r_i and r_j are the radii of the granules i and j, respectively.

In the Hertzian theory of elastic contact for spheres, the spring constant k_n in Eq. (2) is defined as [4,5,18]

$$k_n = \frac{4}{3}\sqrt{\frac{r_i r_j}{r_i + r_j}}\frac{E_i E_j}{(1-\nu_j^2)E_i + (1-\nu_i^2)E_j}, \tag{4}$$

where E and ν are the Young's modulus and the Poisson ratio of the granule, respectively. In the case of contact between a granule and the enclosure wall, k_n can be expressed as

$$k_n = \frac{4\sqrt{r_i}}{3}\frac{E_i E_w}{(1-\nu_w^2)E_i + (1-\nu_i^2)E_w}, \tag{5}$$

where E_w and ν_w denote the Young's modulus and the Poisson ratio of the enclosure wall, respectively.

The determination of the damping force in Eq. (2), on the other hand, has been a constant research issue. In Ref. [14], it was stated that the damping force could be determined heuristically as

$$D_n = \alpha\sqrt{m_i k_n}\delta_{nij}^{1/4}\dot{\delta}_{nij}, \tag{6}$$

where α is a constant coefficient which depends only on the coefficient of restitution e, and $\dot{\delta}_{nij}$ is the normal velocity of granule i relative to granule j. Fig. 2 shows the relation between the parameter α and the coefficient

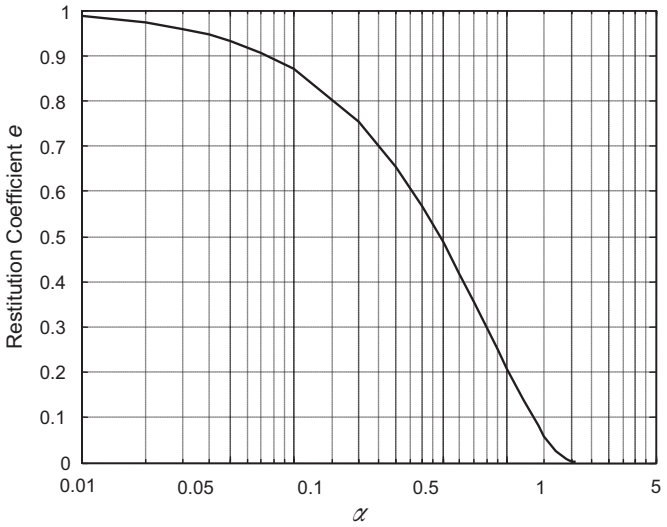

Fig. 2. Relation between the parameter α and the restitution coefficient e (obtained using the approach outlined in Ref. [14]).

of restitution e (obtained using the approach outlined in Ref. [14]). The main advantage of this model is that it reflects the nonlinear impact mechanism while very few empirical coefficients are needed. The tangential component $\boldsymbol{f}_{tij}$ of the contact force can be described using Coulomb's friction [4,5],

$$\boldsymbol{f}_{tij} = -\mu|\boldsymbol{f}_{nij}|\dot{\delta}_{tij}/|\dot{\delta}_{tij}|, \tag{7}$$

where μ is the friction coefficient, and $\dot{\delta}_{tij}$ is the tangential velocity of granule i relative to granule j. In this research, this model will be not only used to calculate the contact force, but also employed to optimize the time step in the discrete element method.

4. Improved discrete element method for granular damping analysis

Section 3 outlines the description of dynamic interactions among granules and between the granules and the wall. A granular damper usually has a large number of granules. Meanwhile, the performance of a granular damper can only be evaluated with sufficiently long simulation time (e.g., a number of periods), which is especially true for structural vibration in the low-frequency range. A major portion of computational cost in the discrete element method is spent on the determination of the contact occurrence in the granular motion. In this section, we present a systematic approach that can significantly improve the contact detection efficiency.

4.1. Enhanced LC method for contact detection in granular vibration

The discrete element method requires the examination of the contacts made by a granule with other granules or with the enclosure wall at each time step during the simulation. In the early work by Cundall and Strack [8], for each granule in the simulation, contact check was performed on all other granules regardless of actual granular motion status, which is of computational complexity $O(n^2)$ at each time step [11,12]. When the number of granules is large, a significant amount of computational time is needed to determine which pairs of granules are in contact, and the overall computation cost becomes extremely high [19]. Clearly, a significant amount of computational effort could be reduced if we can limit the contact examination to a small range. For some granular motion analyses including the granular damping analysis, we may have an important feature, i.e., there is no long-range pairwise interaction, and contact forces only affect the pair of granules that are in direct contact. Currently, many new approaches, such as the LC method, the octree-based detection algorithm, and the spatial digital tree algorithm, have been developed for contact detection [12,19–21]. The LC

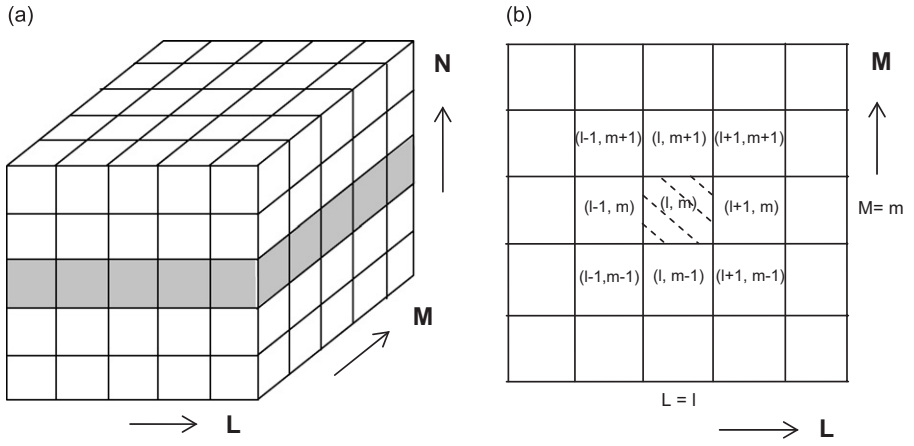

Fig. 3. (a) Subdividing the geometric space into a regular cubic lattice, (b) link cell method. For each cell, there are 26 neighboring cells (8 in this two-dimensional illustration).

method, or referred to as the boxing technique, has been successfully practiced in granular damping analysis [2,3]. The basic idea of the LC method is to partition the enclosure space into a three-dimensional grid of cubic cells and assign each granule to a cell containing its center. As shown in Fig. 3(a), the enclosure is now divided into N_c ($= LMN$) cells, and a two-dimensional slice of the three-dimensional damper enclosure is illustrated in Fig. 3(b). For granular damping analysis, the size of the cell is usually chosen at the same order as the diameter of the granules [3,9]. Therefore, one or more granules can be accommodated to move within each cell. With this cell scheme, only the granules in the same cell or in its 26 neighboring cells (8 in this two-dimensional illustration) need to be checked in order to detect contacts at each time step. The computational complexity to find all the pairs that are in contact now scales as $O(n)$ [11,12].

In this research, we will further improve the LC method for our simulation. In granular damping analysis, it is not uncommon to deal with a large number of granules. However, searching the candidate contacting pairs for a very large n by the LC method is still computationally costly [11,12]. Owing to the nature of contact in a granular damper, the LC method can actually be improved by taking into account the contacting force relation to reduce the number of non-empty cells to be examined, which is stated as follows. Consider a cell ($l-1$, m, n) which contains granule i, as shown in Fig. 4(a) (two-dimensional slice for illustration). In order to find the granules that may be in contact with granule i, we will check the granules in the neighboring cells adjacent to cell ($l-1$, m, n), e.g., cell (l, m, n). If granule j is within the cell (l, m, n), then granular pair ij is a candidate contacting pair and (i,j) will be stored in the neighbor list for the contact force calculation. That is, if the distance between granules i and j is smaller than r_i+r_j, we will calculate the contact force $\boldsymbol{f}_{ij}(\neq 0)$ which is applied by granule j to granule i; otherwise, $\boldsymbol{f}_{ij}=0$. Similarly, when searching for contacts with granule j residing in the cell (l, m, n), as shown in Fig. 4(b), we also have the candidate contacting pair ji. However, since $\boldsymbol{f}_{ji}=-\boldsymbol{f}_{ij}$, there is no need to store (j,i) in the neighbor list. Instead, we only need to record $\boldsymbol{f}_j=\boldsymbol{f}_j-\boldsymbol{f}_{ij}$ in the formulation of the forces loops. In this improved LC procedure, it is only necessary to examine contacts of a granule with other granules in the same cell or its neighboring cells with higher indices. For example, in the two-dimensional slice shown in Fig. 4(a), we perform contact check of granule i with the granules in cells ($l-1$, m), (l, m), ($l-2$, $m+1$), ($l-1$, $m+1$), and (l, $m+1$) only. Meanwhile, for granule j, only the granules in cells (l, m), ($l+1$, m), ($l-1$, $m+1$), (l, $m+1$), and ($l+1$, $m+1$) need to be checked, as shown in Fig. 4(b). Generally, for each cell, there are 13 neighboring cells or less that need to be examined in a three-dimensional case.

4.2. Combining Verlet table with LC method

The spatial distribution of granules constantly changes during the vibration. When the number of the granules n increases, updating the list of candidate pairs in the neighboring cells in the LC method becomes increasingly time consuming. In Ref. [3], the computational time of a granular damper with 936 granules for

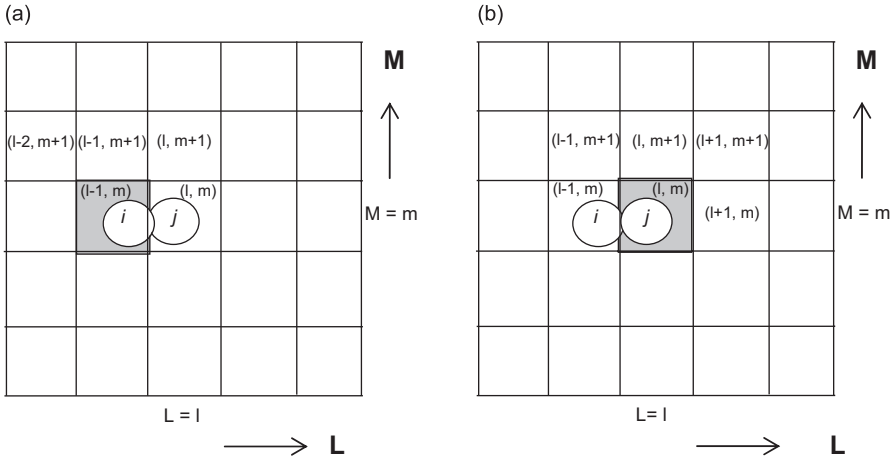

Fig. 4. (a) Contact check of granule i in cell (l−1, m, n) with other neighbor granules, (b) contact check of granule j in cell (l, m, n) with other neighbor granules.

1.5 s free vibration is 5.14 h, while that of a damper with 1246 granules increases to 8.06 h. On the other hand, the time step in the discrete element method simulation is generally small, which means one may be able to avoid updating the neighbor list for each time step. In a molecular dynamics analysis, Verlet [19] pointed out that by using a table recording all granular pairs which are separated by a distance less than r_c+s, where r_c is the cutoff in the range of the interaction potential and s is the thickness of the extra skin, significant reductions in computational time for contact detection could be achieved. In granular damping, since there is no long-range interaction among granules for granular damping analysis, we have $r_c = r_i + r_j$. In the case that all granules have the same radius r, we have $r_c = 2r$. Fig. 5 illustrates, in a two-dimension case, two granules separated by a distance larger than the threshold, although they are in two neighboring cells. The advantage of combining a Verlet table with the link cell method is that it can further reduce the number of candidate pairs by searching for *immediate neighbors* within the threshold distance d_t ($= r_c+s$) [22]. Since the time step Δt is small, the magnitudes of granular displacements are also small during a certain number of time steps [22–24]. Therefore, depending on the dynamic states of the granules, the time step Δt, the size of the cell, and the value of s, the Verlet table recording the immediate neighbor pairs can be updated at a longer time interval. This can greatly reduce the time for determining which pairs are close enough to interact.

The Verlet table, meanwhile, also needs to be updated during the granular motion. Verlet [19] suggested that the interval between updating the table could be fixed at the beginning of the simulation. We may express this updating interval in terms of the number of integration time steps used in the discrete element method, where the time step is related to granular physical properties and collisional velocity, which will be discussed in the next section. In order to guarantee a stable and accurate simulation, the fixed updating interval was usually selected small, e.g., $16 \cdot \Delta t$. In granular damping analysis, the dynamic states of granules, e.g., the velocity and position of each granule, undergo changes after each time step. The updating procedure can be automated by monitoring the dynamic states of granules since the last update of the Verlet table. Fincham and Ralston [23] proposed to update the table when the sum of the magnitudes of the two largest displacements exceeded s. Blink and Hoover [24] used a slightly different procedure and updated the table when the largest displacement exceeded $\sigma[1-1/(n_1+1)]s$, where σ is an empirical factor (e.g. 0.95) and n_1 is the number of time steps since the last update. In those studies, extra computer memories were used to store the displacement information at each time step, and calculating the granule displacements and comparing them with the critical value, for example, s or $\sigma[1-1/(n_1+1)]s$, were computationally expensive, especially when the number of granules is large. In this research, we present a new procedure to adaptively update the Verlet table, which is described as following:

(1) Construct the Verlet table listing the immediate neighbor pairs at the beginning of the simulation.
(2) At the step of constructing or updating the Verlet table, find the maximum velocity $v_{\max}$ among the granules.

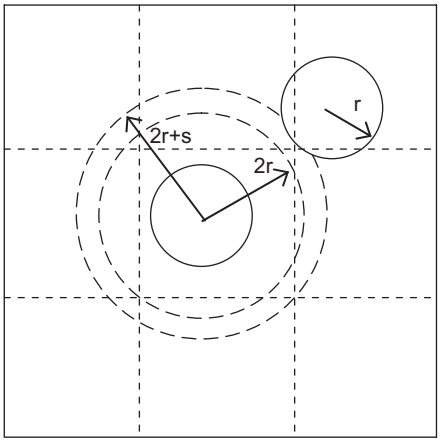

Fig. 5. Two granules in neighboring cells separated by a distance larger than $2r+s$.

(3) Calculate the value of $s/(2\beta v_{\max}\Delta t)$. If $s/(2\beta v_{\max}\Delta t) \leqslant U_L$, the next interval step is selected to be equal to int$[s/(2\beta v_{\max}\Delta t)]$, here β is a safety factor [11] (e.g. 1.5), and U_L is the upper limit value of the interval number; otherwise, the next interval step is equal to U_L.

At the step of updating the Verlet table, $2v_{\max}$ is the possible maximum relative velocity of all the granular pairs. Therefore, $2v_{\max}\Delta t$ is the possible maximum relative displacement of all the pairs in one time step. A pair of granules separated by a distance that is slightly larger than $2r+s$ at current step may become immediate neighbor after a certain time interval. Hence, the next interval step can be estimated as int$[s/(2\beta v_{\max}\Delta t)]$. The safety factor β guarantees that the time interval between updating the Verlet table will not be too long, as an excessively long time interval may result in an inaccurate contact list [11,24]. On the other hand, the larger the safety factor, the smaller the time interval between updating the Verlet table will be, which will decrease the efficiency of the discrete element approach. In practical implementation, this safety factor can be selected based on trial-and-error using a small-scale test run with comparison with respect to the conventional discrete element approach. As will be shown later, in this study we use $\beta = 1.5$, which guarantees both the accuracy and the efficiency of the proposed new approach. In a granular damping analysis, all granules usually rest on the bottom of the enclosure at the initial phase of vibration (i.e., $v_{\max} \approx 0$). To avoid the extremely long interval estimated as int$[s/(2\beta v_{\max}\Delta t)]$, which may result in an unstable simulation, here we introduce the upper limit U_L. In this new procedure, we only need to identify the maximum velocity $v_{\max}$ at the updating step, and we do not need to store and calculate the displacements for updating the table at each time step as practiced in Refs. [23,24]. After all the immediate neighbor pairs are listed, the next step involves the detection of precise contact between them by comparing the distances between those pairs with the corresponding summation of their radii, which is quite straightforward.

4.3. Optimal selection of integration time step

Since a numerical time-integration scheme is used in the discrete element method to solve the equations of motions of granules, the stability and accuracy of the simulation are dependent on the selection of the time step. Generally, the time step should be sufficiently small (smaller than a certain critical value) to make the calculation stable [14,15]. The smaller the time step, the more stable and accurate the calculation is. However, smaller time step also leads to longer computational time. In this section, we present a contact mechanics-based criterion to optimally select the time step.

Because the time step should be small enough to characterize the granular behavior during the contact, we first study the duration time of typical granules when they collide with each other. Consider two identical

granules with the same velocity magnitude colliding with each other, as shown in Fig. 1(a). Here, we use the nonlinear force–displacement model presented in Section 3 to describe the contact mechanics. The physical properties of the two granules are listed in Table 1. Fig. 6 shows the calculated velocity of a granule versus time. At $t = 0$, the granule begins to collide with the other one with incoming velocity 2.5 m/s. After $t = 4.05 \times 10^{-5}$ s, the velocity of the granule becomes a constant -2.244 m/s, which means that the two granules become separated when $t = 4.05 \times 10^{-5}$ s. Thus, the collision duration for this case study is 4.05×10^{-5} s. Fig. 7 shows the collision durations for granules with different sizes and incoming velocities. Clearly, the duration time depends on the size of the granule and the incoming velocity.

In order to completely characterize the granular contact in the discrete element method analysis, the time step in the numerical simulation should be selected as a fraction of the collision duration. An optimal time step should be the one that yields accurate simulation results with minimized simulation time (or, equivalently, maximized time step). We now compare the simulation results under various selections of time steps for a benchmark example. We randomly distribute 300 identical granules in an enclosure of length 25 mm, width 25 mm, and height 35.9 mm, where the properties of granules are listed in Table 1. Each granule has an initial velocity magnitude 2.5 m/s while the direction of the velocity is randomly selected. The numerical accuracy can be examined by comparing the change of overall energy of granules. Since the collisions are inelastic, the overall energy of granules is dissipated if the calculation is stable. The time history of overall energy under various selections of time step is shown in Fig. 8. Here, the time steps are selected as integral fractions (i.e., $4.05 \times 10^{-5}\,\mathrm{k}^{-1}$) of the collision duration. Fig. 8 shows that the result corresponding to $\Delta t = 5.06 \times 10^{-6}$ s (i.e., $k = 8$) is nearly the same as that corresponding to $\Delta t = 2.53 \times 10^{-6}$ s (i.e., $k = 16$). On the other hand, although the overall energy is dissipated in the case of $k = 4$, the energy history is quite different from the case

Table 1
Physical properties of the granules (case study in 4.3)

Diameter $2r$		3 mm
Density		1190 kg/m^3
Spring constant k_n	Granule-to-granule	$1.0 \times 10^7 \sqrt{r/3}$ N/m$^{3/2}$
	Granule-to-wall	$1.3 \times 10^7 \sqrt{r/3}$ N/m$^{3/2}$
Coefficient of friction μ		0.52
Damping constant α		0.077

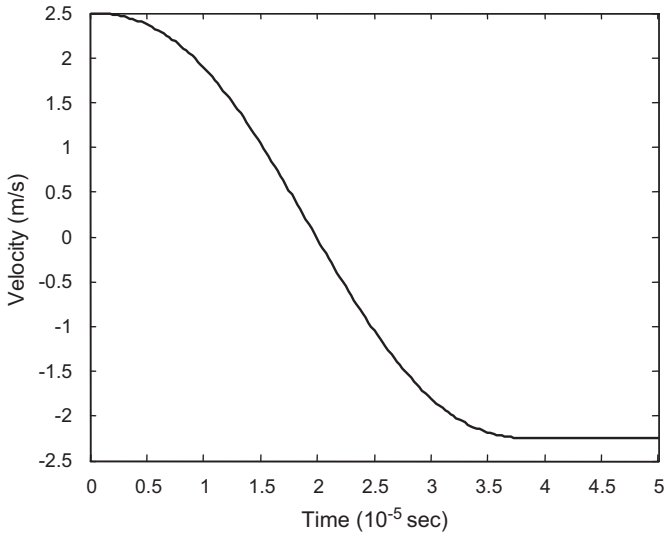

Fig. 6. Result of velocity for inelastic collision with incoming velocity 2.5 m/s.

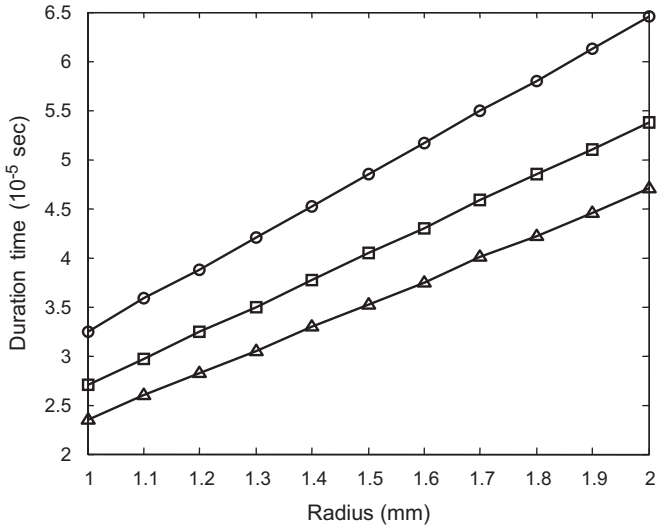

Fig. 7. Contact duration time for granules with different sizes and incoming velocities: ○, 1 m/s; □, 2.5 m/s; △, 5 m/s.

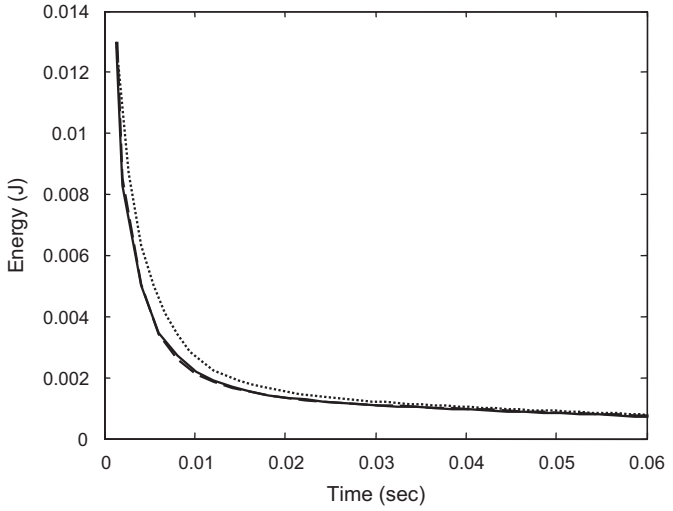

Fig. 8. Energy histories under different time-steps: ⋯⋯, $k = 4$; ——, $k = 8$; — ·, $k = 16$.

of $k = 16$. From this case study, one can easily decide that, for the specific granules discussed in this example, the optimal time step should be selected as 4.05×10^{-5} s/8. Compared with a much smaller time-step 4.05×10^{-5} s/16, this optimal time-step yields the same simulation accuracy but much reduced simulation time. This will be further verified in the case studies presented in Section 5.

A flow chart for the improved discrete element approach proposed in this research is shown in Fig. 9.

5. Case studies for verification and demonstration

In this section, we perform detailed case studies to demonstrate the accuracy and efficiency of the proposed improved discrete element approach. We also use this new approach to explore the energy dissipation mechanisms in a typical granular damper and perform design improvement.

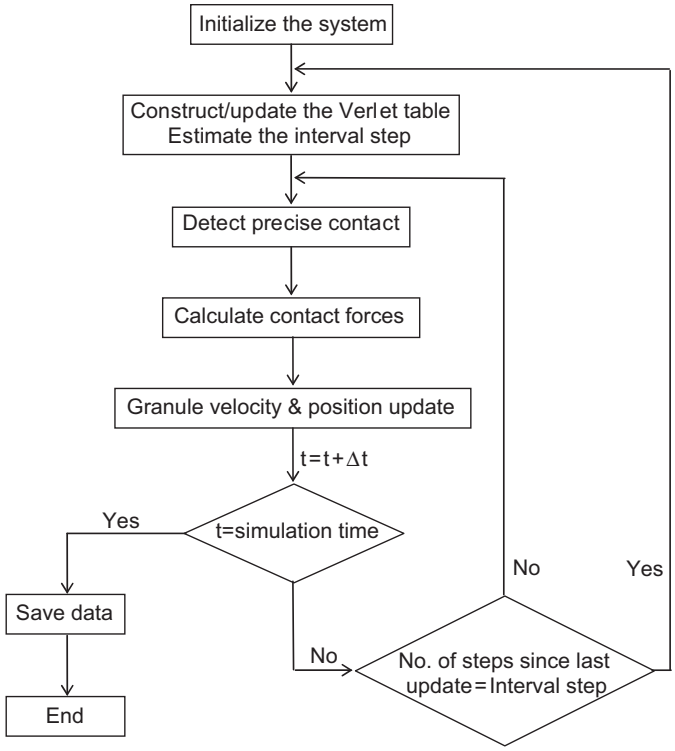

Fig. 9. The flow chart for the DEM simulation.

5.1. *Verification of the improved discrete element approach for granular damping analysis*

A single degree-of-freedom vibrating structure integrated with a granular damper is shown in Fig. 10. The total mass of the structure with enclosure (excluding the granules) is M, and the stiffness and the intrinsic damping are K and c, respectively. In this illustration, the enclosure is a rectangular box with length l, width w, and height h. We first assume that there are n granules of uniform physical properties randomly filled in the enclosure and the total mass of the granules is m. We verify the validity of the improved discrete element approach by comparing the simulation results with existing numerical and experimental results under free and forced vibrations.

In Ref. [2], the transient response of a single-degree-of-freedom structure integrated with granular damper was simulated by the discrete element method, where a conventional LC method was implemented in contact detection. The structure/enclosure has an initial displacement 15.7 mm with zero velocity. In our simulation, the parametric settings are the same as those used by in Ref. [2] (see Table 2). The simulation results of free vibration velocities with and without the granular damper are shown in Fig. 11(a). We also plot the specific damping capacity, which is defined as the ratio of the kinetic energy of the structure dissipated during one cycle of vibration to the maximum kinetic energy of the structure during that cycle [1,2] (Fig. 11(b)). Clearly, both the velocity profile and the energy dissipation history obtained using the proposed approach have good agreement with those given in Ref. [2]. The slight difference in damping capacity prediction is due to the difference in initial granular distribution configuration, which plays an important role in this specific case of transient analysis. The energy dissipation level has obvious amplitude dependency.

We further verify the improved discrete element approach with the experimental results given by Saeki [4], where a single degree-of-freedom system vibrating horizontally under harmonic excitation is analyzed. One may refer to [4] for the details of the experimental set-up, and the relevant simulation parameters are listed in Table 3. The structure/enclosure is subject to a harmonic excitation $F(t) = Ka \sin 2\pi ft$ in the experiment, where a is known as the static deflection, and f is the excitation frequency. In Ref. [4], Saeki obtained experimentally

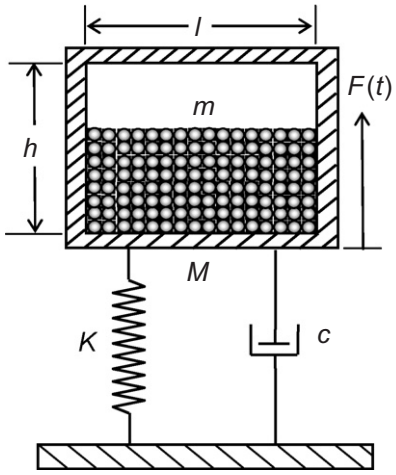

Fig. 10. Sketch of a single-degree-of-freedom system with granular damping.

Table 2
Parameters used in DEM verification under free vibration (case study in 5.1 and 5.2)

System parameter		Granular simulation parameter	
Mass M	0.0376 kg	Normal stiffness	360 kN/m$^{3/2}$
Mass m	0.0004 kg	Normal damping	0.01 N s/m
Stiffness K	1410 N/m	Tangential stiffness	330 kN/m$^{3/2}$
Damping c	0.1 N s/m	Tangential damping	0.015 N s/m
Cylinder hole diameter	5.25 mm	Coefficient of friction	0.55
Cylinder hole height	8.84 mm	Granule diameter $2r$	0.88 mm
		Granule number n	130

the root mean square value of the primary system amplitude versus the excitation frequency f for $a = 1$ mm. A comparison of the experimental result and the numerical result obtained by the method proposed in this paper is given in Fig. 12, which indicates a complete agreement. The granular damping can indeed suppress structural vibrations over a wide frequency range. For a very small weight penalty ($m/M = 0.092$), the resonant amplitude of the primary system is reduced by nearly 90%. The reduced peak amplitude of the primary system with granular damping now occurs at a lower frequency compared with that without the granular damper, due to the added mass of granules. It is worth mentioning that in the above simulations, the time step is selected according to the optimal criterion given in Section 4.3.

5.2. *Efficiency demonstration of improved discrete element method approach*

The above case studies demonstrate the accuracy and effectiveness of the improved discrete element approach. In this section, we focus on the computational efficiency of the discrete element method simulation by a series of comparative studies. In Ref. [3], the computational complexity of the discrete element method simulation was studied with respect to granular density, which was defined as the ratio of the number of granules to the volume of the enclosure. The enclosure's size and the total mass of the granules remained the same while the number of granules and the granule diameter were changed. In our analysis, for a fair comparison, we use the same parametric settings as in Ref. [3]. In fact, most of the parameters are the same as shown in Table 2, whereas the enclosure diameter and height are changed to 10 and 24.64 mm, respectively, to accommodate more granules in this case study. The number of granules ranges from 300 to 1300. The initial displacement of the system is assumed to be 15.7 mm, and the initial velocity is zero. In Ref. [3], the conventional LC method is implemented for the granule contact detection. In our simulation, we implement

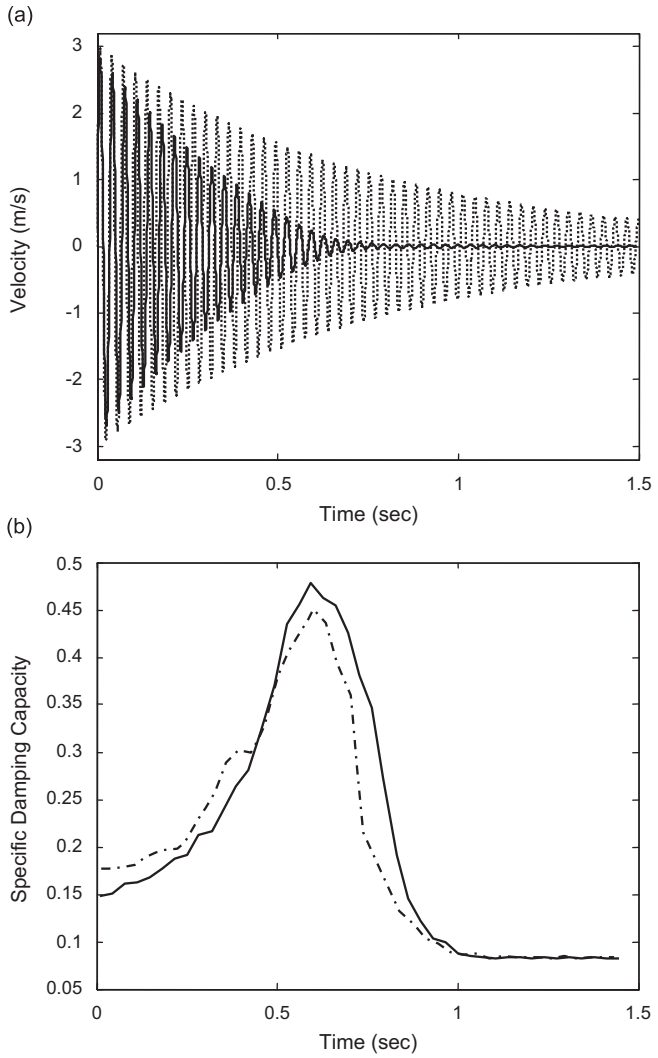

Fig. 11. (a) DEM simulation result of free vibration velocity responses with and without granules: ——, with granules; ·····, without granules; (b) specific damping capacity of the system with granules: ——, improved DEM developed in this research; – · – · –, DEM result reported in Ref. [2].

Table 3
Parameters used in DEM verification under forced vibration (case study in 5.1)

System parameter		Granular simulation parameter	
Mass M	0.293 kg	Granule–granule normal stiffness	1.0×10^7 N/m$^{3/2}$
Mass m	0.027 kg	Granule–wall normal stiffness	1.3×10^7 N/m$^{3/2}$
Stiffness K	1602.7 N/m	Coefficient of restitution	0.89
Damping c	0.116 N s/m		
Enclosure length l	58 mm	Coefficient of friction	0.52
Enclosure width w	38 mm	Granule diameter $2r$	6 mm
Enclosure height h	38 mm	Granule number n	200

the improved LC method combined with the adaptively updated Verlet table. We select the length of cell as $1.2d$, skin thickness $s = 0.1d$, safety factor $\beta = 1.5$, and the upper limit value of updating interval $U_L = 150$. For comparison purpose, all the simulations are run on a personal computer with a 1.70-GHz Intel Pentium

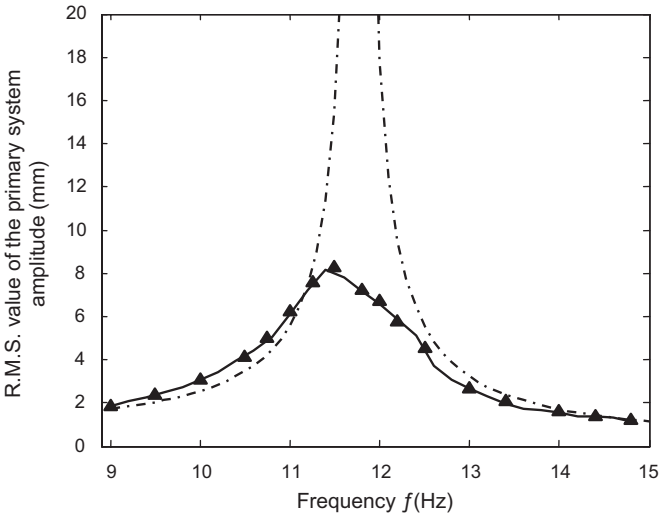

Fig. 12. Comparison between experimental and DEM results ($l = 58$ mm, $w = h = 38$ mm, $r = 3$ mm, and $a = 1$ mm): – · – · –, no damper; ——, experiment; ▲, DEM.

Table 4
Efficiency of the improved DEM algorithm over the conventional LC method (case study in 5.2)

N	Computing time (h)		Efficiency ratio
	Ref. [3]	This work	
312	1.000	0.086	11.6
624	2.873	0.231	12.4
936	5.151	0.357	14.4
1246	8.064	0.545	14.8

processor, which is the same as that used in Ref. [3]. The total computational time to simulation the motion of the system for 1.5 s under different numbers of granules is listed in Table 4. As the number of granules increases, the computational effort increases drastically under the approach used in Ref. [3]. In comparison, the computational time of the proposed approach is one order-of-magnitude lower. Also as shown in Table 4, with the increase of the number of granules, the efficiency ratio of the proposed new algorithm to the one used in Ref. [3] also increases. This clearly indicates that the advantage of the new approach becomes more significant when a larger number of granules are involved.

The efficiency of the improved link cell method combined with the adaptively updated Verlet table is also illustrated in Fig. 13, where we compare the proposed contact detection algorithm with the straightforward search and the improved link cell method without a Verlet table, respectively. Again, the proposed contact detection algorithm greatly outperforms the other two. For example, in the case of $n = 1200$, the average CPU times per simulation step for the straightforward search, the improved link cell method without a Verlet table, and the proposed new approach are 9.375×10^{-3}, 1.458×10^{-3}, and 5.030×10^{-4} s, respectively. Indeed, the proposed new algorithm runs nearly 18.6 times faster than the straightforward search, and 6.4 times faster than the improved link cell method without a Verlet table. Fig. 14 shows the interval steps to update the Verlet table for $n = 450$ during the simulation. At the beginning of vibration, all the granules have nearly zero velocity. In order to avoid extremely long interval, the upper limit value of update interval U_L is chosen to be 150. As shown in Fig. 14, the interval is adaptively changed during vibration. Fig. 15 shows the number of contacts for the case of 450 granules within the period of 1–2 s checked by the straightforward search and the

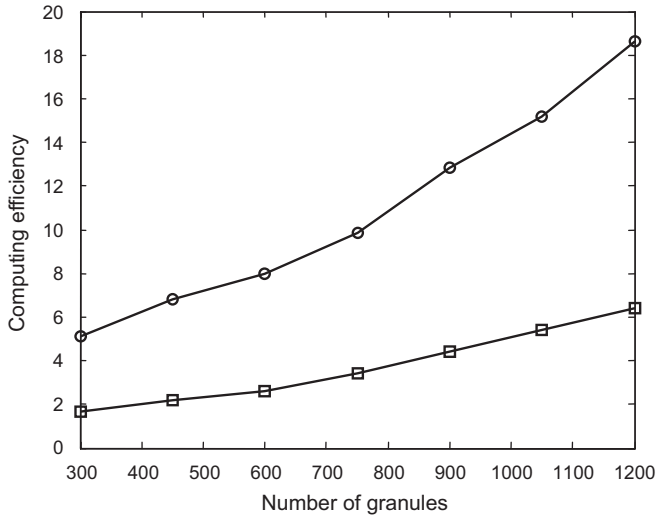

Fig. 13. Efficiency comparison: ○, the proposed approach over the straightforward search; □, the proposed approach over improved link cell method without a Verlet table.

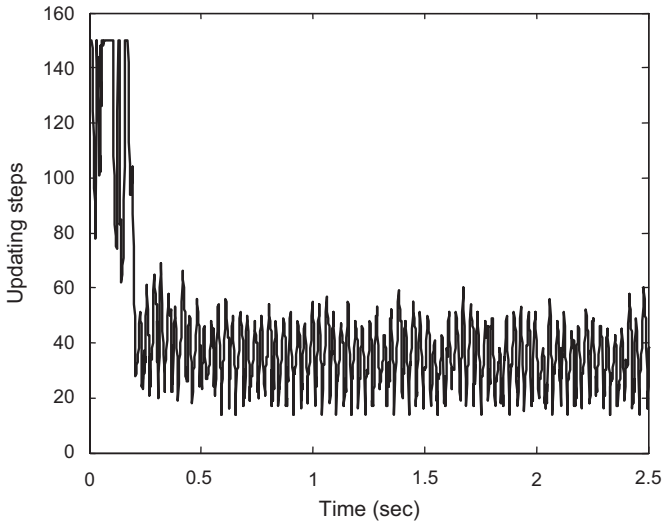

Fig. 14. Adaptively changed interval steps to update the Verlet table during vibration.

improved algorithm, respectively. It can be easily seen from Fig. 15 that the result of the improved algorithm agrees with that of the straightforward search very well. Clearly, the proposed contact detection procedure significantly reduces the computational cost while maintaining the detection accuracy.

5.3. *Damping case studies and performance optimization*

Granular damping is highly nonlinear, and the damping performance depends on a large number of system parameters as well as operating conditions. Usually, the damping performance optimization requires a very large number of simulations/analyses using the discrete element method, which is indeed the motivation for the development of the proposed new algorithm. In this section, we perform damping effect case studies and illustrate the performance improvement based on parametric analyses. Here, we investigate the dynamic

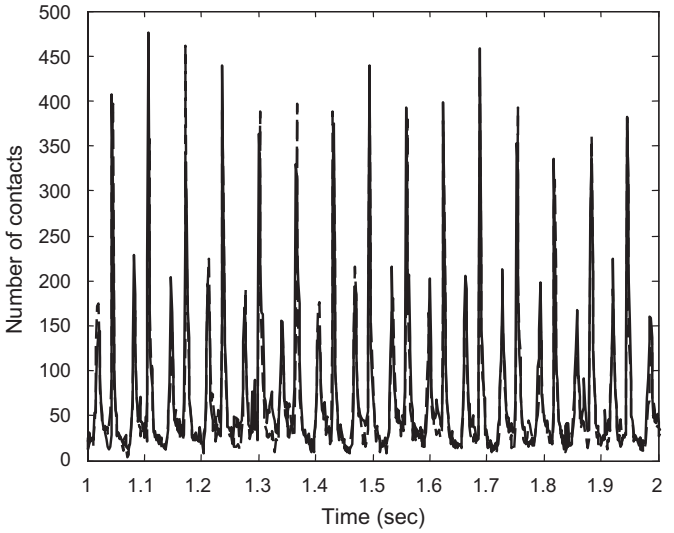

Fig. 15. Number of contacts of 450 granules: —, straightforward search; – · – · –, improved algorithm.

Table 5
Parameters used in parametric analyses (case study in 5.3)

System parameter		Granular simulation parameter	
Mass M	0.1 kg	Granule–granule normal stiffness	$1.0 \times 10^7 \sqrt{r/3}\,\mathrm{N/m^{3/2}}$
Mass m	0.01 kg	Granule–wall normal stiffness	$1.3 \times 10^7 \sqrt{r/3}\,\mathrm{N/m^{3/2}}$
Stiffness K	1000 N/m	Coefficient of restitution	0.89
Damping c	0.2 N s/m		
Enclosure length l	25 mm	Coefficient of friction	0.52
Enclosure width w	25 mm	Granule diameter $2r$	3.7 mm
Enclosure height h	35.9 mm	Granule number n	317

response of a structure integrated with granular damper under the harmonic force excitation. The parameters for the forced vibration simulation are listed in Table 5.

Fig. 16 shows the simulation results of the forced vibration amplitudes of the primary mass with and without granular damping. It should be noted that the excitation frequency f ($= 15.91$ Hz) is equal to the resonant frequency of the system without granules. Without the granular damping, the average peak amplitude of the steady-state response is 24.76 mm. After we implement the granular damping, the average peak amplitude predicted by the discrete element method simulation is 4.63 mm, which represents an 81.3% reduction. Clearly, the granular damper can provide significant damping capacity to suppress the vibration. The behaviors of the system with or without granular damping, presented as frequency response functions, are shown in Fig. 17. For all responses, the simulations are run for 7 s of vibration to allow the transients to die out. Over the frequency range 15.5–16.5 Hz, the forced responses with granular damping are reduced by 39.4–81.3% compared with those without granular damping. The granular damper can attenuate structural vibration over a wide frequency range. It is worth mentioning that the resonant frequency of the vibrating system with the granular damper falls in between the resonant frequency of the system without the granular damper and that with the granules being just an added mass to the primary mass. The reason is that during the vibration the granules alternate from the state of being in contact with the structure/enclosure to the state of being separated from the enclosure/structure.

Under a specific operating condition, the granular damping performance can be optimized by adjusting the size/number of the granules with the total mass of the granules being kept as constant. In the following analysis, the structure/enclosure is subject to a harmonic excitation $F(t) = Ka \sin 2\pi ft$, where $a = 0.5$ mm and

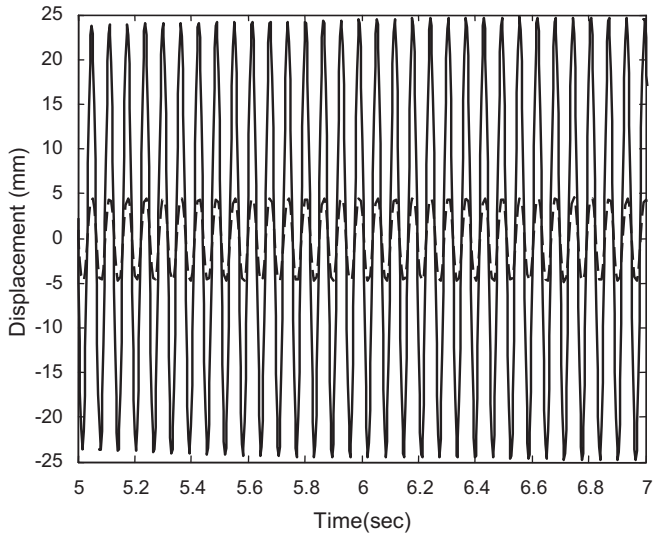

Fig. 16. Forced response of the primary structure when $a = 0.5$ mm, and $f = 15.91$ Hz: ——, without granular damping; — —, with granule damping.

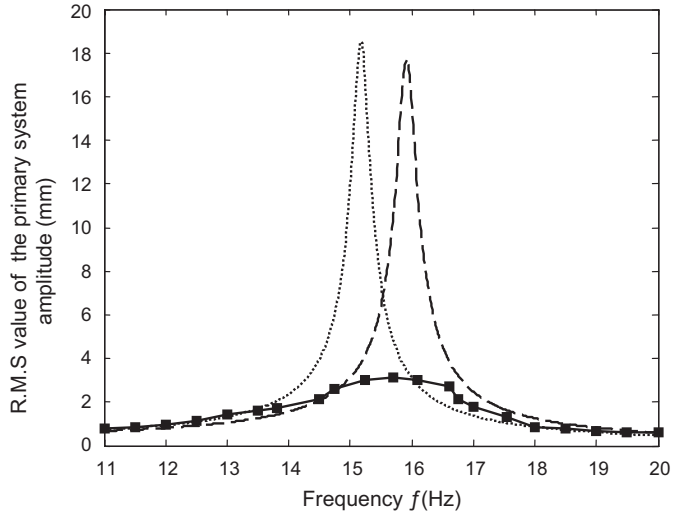

Fig. 17. Frequency responses when $a = 0.5$ mm: — —, no damper; ·····, added mass only; —■—, DEM.

$f = 15.5$ Hz. The total mass of the granules is kept at 0.01 kg and the number of granules and the granule diameter are varied, whereas all other simulation parameters are the same as those given in Table 5. In Fig. 18, we plot the root mean square value of the primary system amplitude with different numbers of granules (128–2007). It is worth mentioning that with the improved discrete element approach, it only takes 4.07 h to finish the simulation for 7 s of system vibration, for the case where $N = 2007$. From Fig. 18, one can see that when $r = 1.6$ mm (i.e., $n = 490$), the granular damping reaches the maximum. As the number of granules increases or decreases from 490, the granular damping effect decreases. From a mechanistic standpoint, the energy dissipated by granular damping is caused by the impact collisions among the granules and between the granules and the enclosure wall. With more granules, the number of contacts generally increases. The total energy dissipated, nevertheless, is related to not only the number of contacts but also the energy dissipation per contact. It can be easily envisioned that the energy dissipation due to a single granule-to-granule collision or granule-to-wall collision also changes with the size of the granules. Indeed, the values of total work done by

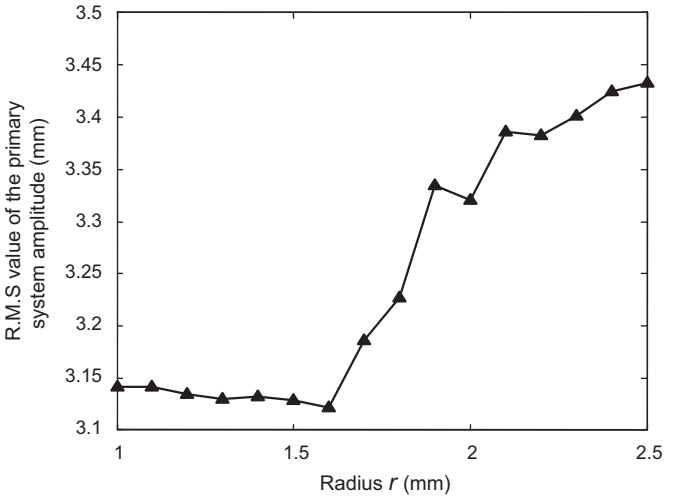

Fig. 18. Forced response of the primary structure with granule damping when $a = 0.5$ mm and $f = 15.5$ Hz.

Table 6
Forced responses of the primary system with different sizes and numbers of granules (case study in 5.3)

Granule 1		Granule 2		Root mean square (mm)
r_1 (mm)	n_1	r_2 (mm)	n_2	
1.6	490			3.122
1.6	350	1.2	332	3.129
1.6	350	1.4	209	3.081
1.6	350	1.8	98	3.205
1.6	350	2.0	72	3.214

the external excitation force for the three cases studied ($r = 1$, 1.6, and 2.5 mm) for 7 s simulation are 1.453, 1.450, and, 1.481 J, respectively, while the corresponding energy dissipated by granular damping are 1.228, 1.237, and 1.105 J, respectively. Therefore, the values of average energy dissipated by a single granule for these three cases are 6.12×10^{-4}, 2.52×10^{-3}, and 8.63×10^{-3} J, respectively, which show significant difference. In summary, the total energy dissipated is related to the number of contacts as well as energy dissipation per contact, and a trade-off can be found for damping optimization. Under the given operating condition, when $n = 490$, the damper appears to have the maximum damping capacity and the root mean square value of the primary system amplitude is 3.122 mm.

The above analysis actually implies one possibility of further improving the damping performance, i.e., using multiple sizes of granules within the damper enclosure. Here, we consider the case with two sizes of granules mixed together, where the total mass of the granules is still kept as 0.01 kg. Table 6 lists the forced response of the primary system with different scenarios of mixed granular sizes. From this table, we can see the forced response of the primary system with the following two sizes of granules, $r_1 = 1.6$ mm (Type 1, $n_1 = 350$) and $r_2 = 1.4$ mm (Type 2, $n_2 = 209$), is further reduced from that with only one size $r_1 = 1.6$ mm ($n_1 = 490$). In this case study, the size of Type 2 granules is only slightly smaller than that of Type 1 granules. Therefore, under the same excitation, the average energy dissipated by a single Type 2 granule will be comparable with that by a single Type 1 granule. However, mixing Type 1 granules with slightly smaller Type 2 granules while maintaining the total added mass can significantly increase the total number of granules (from 490 to 559) and hence the number of contacts amongst granules and between the granules and the enclosure wall increases. As a result, the total energy dissipated by a damper with the two sizes of granules ($r_1 = 1.6$ mm and $r_2 = 1.4$ mm) is larger than that by a single size of granules ($r_1 = 1.6$ mm) (see Table 6). This comparative study clearly

indicates that with a proper selection of the sizes of mixed granules the damping performance can be further improved. All these analyses are performed by using the improved discrete element approach. Indeed, granular damping analysis is very intriguing and usually a large number of parametric studies are needed for damping optimization. The proposed improved discrete element approach can serve as a powerful tool for practical applications.

6. Concluding remarks

A new computational scheme for granular damping analysis using the discrete element method is developed. To increase the contact detection efficiency, an algorithm that combines an improved LC method and an adaptively updated Verlet table is explored. We also study the effect of time step in simulation, and develop a procedure that can optimize the time-step selection based on the contact duration of given granules. Collectively, these improvements yield a highly efficient discrete element algorithm that can increase the computational efficiency of granular damper analysis by multiple times as compared to the state-of-the-art. This new algorithm is especially suitable for granular damping analysis involving large number of granules. This approach is validated by correlating to benchmark numerical and experimental results. With the new algorithm as basis, case studies on large number of granules are carried out to illustrate the parametric analysis of granular damping mechanisms and the damping performance improvement.

Acknowledgment

This research was supported by the National Science Foundation under Grant CMS-0324436.

References

[1] R.D. Friend, V.K. Kinra, Particle impact damping, *Journal of Sound and Vibration* 233 (1) (2000) 93–118.
[2] K.M. Mao, M.Y. Wang, Z.W. Xu, T.N. Chen, Simulation and characterization of particle damping in transient vibration, *Journal of Vibration and Acoustics—Transactions of the ASME* 126 (2) (2004) 202–211.
[3] K.M. Mao, M.Y. Wang, Z.W. Xu, T.N. Chen, DEM simulation of particle damping, *Powder Technology* 142 (2004) 154–165.
[4] M. Saeki, Impact damping with granular materials in a horizontally vibration system, *Journal of Sound and Vibration* 251 (1) (2002) 153–161.
[5] M. Saeki, Analytical study of multi-particle damping, *Journal of Sound and Vibration* 281 (1) (2005) 1133–1144.
[6] E.M. Flint, Experimental measurements of the particle damping effectiveness under centrifugal loads, *Proceedings of the Fourth National Turbine Engine High Cycle Fatigue Conference*, Monterey, California, February 9–11, 1999.
[7] B.L. Fowler, E.M. Flint, S.E. Olson, S. E., Effectiveness and predictability of particle damping, *Proceedings of SPIE Conference on Smart Structures and Materials: Damping and Isolation,* Newport Beach, California, March 2000, pp. 356–367.
[8] P. Cundall, O. Strack, A distinct element model for granular assemblies, *Geotechnique* 29 (1979) 47–65.
[9] E. Tijskens, H. Ramon, J.D. Baerdemaeker, Discrete element modeling for process simulation in agriculture, *Journal of Sound and Vibration* 266 (2003) 493–514.
[10] T. Chen, K. Mao, X. Huang, M.Y. Wang, Dissipation mechanisms of non-obstructive particle damping using discrete element method, *Proceedings of SPIE International Symposium on Smart Structures and Materials: Damping and Isolation,* Newport Beach, California, March 2001, pp. 294–301.
[11] G.S. Grest, B. Dunweg, K. Kremer, Vectorized link cell Fortran code for molecular dynamics simulations for a large number of particles, *Computer Physics Communications* 55 (1989) 269–285.
[12] B.C. Vemuri, L. Chen, Q.L. Vu, X. Zhang, O. Walton, Efficient and accurate collision detection for granular flow simulation, *Graphical Models and Image Processing* 60 (1998) 403–422.
[13] G.A. Bird, *Molecular Gas Dynamics and the Direct Simulation of Gas Flows*, Oxford Science Publications, Oxford, 1994.
[14] Y. Tsuji, T. Tanaka, T. Ishida, Lagrangian numerical simulation of plug flow of cohesionless particles in a horizontal pipe, *Powder Technology* 71 (1992) 239–250.
[15] Y. Tsuji, T. Kawaguchi, T. Tanaka, Discrete particle simulation of two-dimensional fluidized bed, *Powder Technology* 77 (1993) 79–87.
[16] D. Zhang, W.J. Whiten, The calculation of contact forces between particles using spring and damping models, *Powder Technology* 88 (1996) 59–64.
[17] B.K. Mishra, C.V.R. Murty, On the determination of contact parameters for realistic DEM simulations of ball mills, *Powder Technology* 115 (2001) 290–297.
[18] K.L. Johnson, *Contact Mechanics*, Cambridge University Press, Cambridge, 1985.

[19] L. Verlet, Computer experiments on classical fluids. I. Thermodynamical properties of Lennard–Jones molecules, *Physical Review* 159 (1967) 98–103.
[20] J.R. Williams, R. O'Connor, Discrete element simulation and the contact problem, *Archives of Computational Methods in Engineering* 6 (4) (1999) 279–304.
[21] Y.T. Feng, D.R.J. Owen, An augmented spatial digital tree algorithm for contact detection in computational mechanics, *International Journal for Numerical Methods in Engineering* 55 (2002) 159–176.
[22] M.P. Allen, D.J. Tildesley, *Computer Simulation of Liquids*, Clarendon Press, Oxford, 1987.
[23] D. Fincham, B.J. Ralston, Molecular dynamics simulation using the Cray-1 vector processing computer, *Computer Physics Communications* 23 (1981) 127–134.
[24] J.A. Blink, W.G. Hoover, Fragmentation of suddenly heated liquids, *Physical Review A* 32 (1985) 1027–1035.